Resolvin D1 and Its Aspirin-triggered 17r Epimer. Stereochemical Assignments, Anti-inflammatory Properties, and Enzymatic Inactivation

THE JOURNAL OF BIOLOGICAL CHEMISTRY VOL. 282, NO. 13, pp. 9323–9334, March 30, 2007

Resolvin D1 and Its Aspirin-triggered 17*R* Epimer

*STEREOCHEMICAL ASSIGNMENTS, ANTI-INFLAMMATORY PROPERTIES, AND ENZYMATIC INACTIVATION**

Received for publication, September 28, 2006, and in revised form, December 22, 2006 Published, JBC Papers in Press, January 23, 2007, DOI 10.1074/jbc.M609212200

Yee-Ping Sun[‡], Sungwhan F. Oh[‡], Jasim Uddin[§], Rong Yang[‡], Katherine Gotlinger[‡¶], Eric Campbell[‡], Sean P. Colgan[‡], Nicos A. Petasis[§], and Charles N. Serhan[‡¶1]

From the [‡]Center for Experimental Therapeutics and Reperfusion Injury, Department of Anesthesiology, Perioperative and Pain Medicine, Brigham and Women's Hospital and [¶]Department of Oral Medicine, Infection and Immunity, Harvard School of Dental Medicine and Harvard Medical School, Boston, Massachusetts 02115 and the [§]Department of Chemistry, Loker Hydrocarbon Institute, University of Southern California, Los Angeles, California 90089

We recently uncovered two new families of potent docosahexaenoic acid-derived mediators, termed D series resolvins (Rv; resolution phase interaction products) and protectins. Here, we assign the stereochemistry of the conjugated double bonds and chirality of alcohols present in resolvin D1 (RvD1) and its aspirin-triggered 17*R* epimer (AT-RvD1) with compounds prepared by total organic synthesis. In addition, docosahexaenoic acid was converted by a single lipoxygenase in a "one-pot" reaction to RvD1 *in vitro*. The synthetic compounds matched the physical and biological properties of those enzymatically generated. RvD1 proved to be 7*S*,8*R*,17*S*-trihydroxy-4*Z*,9*E*,11*E*,13*Z*,15*E*,19*Z*-docosahexaenoic acid, AT-RvD1 matched 7*S*,8*R*,17*R*-trihydroxy-4*Z*,9*E*,11*E*,13*Z*,15*E*,19*Z*-docosahexaenoic acid, and they both stopped transendothelial migration of human neutrophils (EC_{50} ~30 nM). In murine peritonitis *in vivo*, RvD1 and AT-RvD1 proved equipotent (at nanogram dosages), limiting polymorphonuclear leukocyte infiltration in a dose-dependent fashion. RvD1 was converted by eicosanoid oxidoreductase to novel 8-oxo- and 17-oxo-RvD1 that gave dramatically reduced bioactivity, whereas enzymatic conversion of AT-RvD1 was sharply reduced. These results establish the complete stereochemistry and actions of RvD1 and AT-RvD1 as well as demonstrate the stereoselective basis for their enzymatic inactivation. RvD1 regulates human polymorphonuclear leukocyte transendothelial migration and is anti-inflammatory. When its carbon 17*S* alcohol is enzymatically converted to 17-oxo-RvD1, it is essentially inactive, whereas the 17*R* alcohol configuration in its aspirin-triggered form (AT-RvD1) resists rapid inactivation. These results may contribute to the beneficial actions of aspirin and ω-3 fish oils in humans.

Lipids, like proteins and carbohydrates, are an essential component of the human diet. Observations first reported by Burr and Burr in 1929 demonstrated that exclusion of dietary lipids resulted in multiorgan pathology and premature death (1). Since these early studies, it has become clear that lipids and lipid-derived local chemical mediators play critical regulatory roles in a variety of cellular functions, including inflammation (2). Inflammation is a fundamental component of host defense, because the immune response is responsible for the clearance of injurious agents as well as the associated damaged tissue. In normal physiological states, the inflammatory response is cleared to allow for resolution back to the non-inflamed state to maintain tissue homeostasis (3). Recently, we identified molecular circuits involved in the promotion of this inflammatory resolution and uncovered novel families of ω-3 EPA[2]- and DHA-derived local mediators, named resolvins and protectins (4–6). Defects in these clearance mechanisms appear to be associated with persistent tissue inflammation and autoimmunity to cellular contents (for recent review, see Ref. 7).

It was first observed nearly 30 years ago that a diet enriched in fish oil (of which ω-3 fatty acids are the primary component) is associated with a lower risk of cardiovascular disease (8). Since that report, it is widely discussed that essential ω-3 fatty acids are critical to cellular function and human health (reviewed in Ref. 9). Several studies demonstrated the beneficial effects of ω-3 supplementation in pathological states, including Crohn's disease (10), coronary heart disease (11), and sudden cardiac death (12). Although the clinical findings suggest a benefit from ω-3 supplementation, the molecular mechanisms underlying this protective action have only begun to be uncovered.

The two main ω-3 fatty acids present in fish oil are eicosapentaenoic acid (EPA, C20:5) and docosahexaenoic acid (DHA, C22:6). DHA is highly enriched in both the retina and neuronal synaptic membranes and is a critical component in neural

* This work was supported by National Institutes of Health Grants GM38765, DK074448, and P50-DE016191. The costs of publication of this article were defrayed in part by the payment of page charges. This article must therefore be hereby marked "*advertisement*" in accordance with 18 U.S.C. Section 1734 solely to indicate this fact.

[1] To whom correspondence should be addressed: Center for Experimental Therapeutics and Reperfusion Injury, Dept. of Anesthesiology, Perioperative and Pain Medicine, Brigham and Women's Hospital, 75 Francis St., Boston, MA 02115. Tel.: 617-732-8822; Fax: 617-582-6141; E-mail: cnserhan@zeus.bwh.harvard.edu.

[2] The abbreviations used are: EPA, eicosapentaenoic acid; AT-RvD1, aspirin-triggered RvD1, 7*S*,8*R*,17*R*-trihydroxy-4*Z*,9*E*,11*E*,13*Z*,15*E*,19*Z*-docosahexaenoic acid; DHA, docosahexaenoic acid; GC-MS, gas chromatography-mass spectrometry; LC-MS/MS, liquid chromatography-tandem mass spectrometry; LOX, lipoxygenase; PMN, polymorphonuclear leukocyte; RP-HPLC, reversed-phase high-pressure liquid chromatography; Rv, resolvin, resolution phase interaction product; RvD1, 7*S*,8*R*,17*S*-trihydroxy-4*Z*,9*E*,11*E*,13*Z*,15*E*,19*Z*-docosahexaenoic acid; RvD2, 7*S*,16*R*,17*S*-trihydroxydocosa-4*Z*,8*E*,10*Z*,12*E*,14*E*,19*Z*-hexaenoic acid; EOR, 15-prostaglandin dehydrogenase/eicosanoid oxidoreductase; MPO, myeloperoxidase; HMEC, Human microvascular endothelial cell; HBSS, Hanks' balanced salt solution; fMLP, *n*-formylmethionylleucylphenylalanine; LX, lipoxin.

development (reviewed in Ref. 13). The structures and potential bioactions of putative oxidative products of DHA have been discussed (13, 14) yet remain to be established.

The resolvins (resolution phase interaction products) are a novel family of lipid mediators derived from both EPA and DHA (4, 5, 15). These potent lipid mediators are not only anti-inflammatory but also promote resolution back to the non-inflamed state (6). The identification of the resolvins and protectins as well as their arachidonic acid (C20:4)-derived cousins, lipoxins (LXs), as endogenous stop signals in inflammation provides evidence that resolution is a biochemically active process (4) and not passive as was once believed (3).

DHA is converted through a series of enzymatic oxygenations to both protectins and D series resolvins. Resolvin D1 (RvD1, 7*S*,8*R*,17S-trihydroxy-DHA) is produced in resolving exudates *in vivo* and is a product of transcellular biosynthesis with human leukocytes and endothelial cells (5). RvD1 was also identified in activated human whole blood and murine brain (15) as well as in fish (16). RvD1 biosynthesis involves sequential oxygenations by 15-lipoxygenase (LOX) and 5-LOX (Fig. 1*A*) (15). DHA is converted by 15-LOX to 17*S*-hydroxy-DHA (HDHA). In the case of aspirin treatment, aspirin-acetylated cyclooxygenase-2 generates 17*R*-HDHA, which following sequential oxygenation by 5-LOX results in production of 17-epi-RvD1, also known as aspirin-triggered RvD1 (AT-RvD1) (5, 17, 18).

Both the 17*R* and 17*S* D series resolvins exhibit potent anti-inflammatory action *in vivo* (15), and the recent evidence that trout brain cells also produce RvD1 from endogenous stores of DHA (16) indicates that the RvD1 structure is evolutionarily conserved. These findings, along with the extensive literature surrounding the importance of DHA in neural development and function (14, 19), highlight the need for establishing the complete stereochemistry of both RvD1 and AT-RvD1. Here, we report the complete stereochemistry, anti-inflammatory properties, and enzymatic inactivation of RvD1 and its aspirin-triggered isomer (AT-RvD1).

EXPERIMENTAL PROCEDURES

Mediator Lipidomics—LC-MS/MS-based mediator lipidomic analyses were performed as in previous studies (20, 21). Briefly, sample analyses were carried out using a Finnigan LCQ LC ion trap tandem mass spectrometer equipped with a Thermoelectron BDS Hypersil C18 (100 mm × 2.1 mm × 5 μm) column (Fig. 2) or a Phenomenex C18 (150 mm × 2 mm × 5 μm) column equipped with a rapid spectra scanning UV diode array detector. For routine analyses, the mobile phase (methanol:water:acetic acid, 65:35:0.01) was eluted at a 0.2 ml/min flow rate, and UV spectra were recorded ~0.1 min before samples entered MS/MS. For results in Table 1, spectra were recorded in methanol using a Hewlett-Packard 8453 UV spectrophotometer with accuracy ± 2 nm.

RP-HPLC—Liquid chromatographic analyses were performed using a Hewlett-Packard Series 1100 high-pressure liquid chromatography (HPLC) system equipped with a Phenomenex C18 (150 × 2 mm × 5 μm) column with a UV diode array detector. Matching of synthetic with biological and biogenic materials was carried out with the mobile phase (methanol:water:acetic acid, 70:30:0.01) at a 0.2 ml/min flow rate. RvD1 and AT-RvD1 as well as analysis of the oxo-containing products were performed using a mobile phase (methanol:water:acetic acid, 65:35:0.01) with a 0.2 ml/min flow rate.

GC-MS Analysis—Samples were taken to dryness using a stream of N_2, suspended in MeOH (10 μl), and treated with excess ethereal diazomethane (45 min at room temperature), followed by *N*,*O*-bis(trimethylsilyl)trifluoroacetamide) treatment (overnight at room temperature, obtained from Pierce) (22). GC-MS analysis was performed with a Hewlett-Packard 5971A mass-selective quadrupole detector equipped with an HPG1030A workstation and HP6890 GC system. Samples were injected with hexane as the solvent and the temperature program was initiated at 150 °C and held for 2 min and reached 230 °C at 10 min (10 °C/min) and then 280 °C at 20 min (5 °C/min). Reference saturated fatty acid methyl esters carbons C_{14}-C_{24} gave the following retention times (min, mean of $n = 3$): C_{14}, 6.5; C_{16}, 8.5; C_{18}, 10.4; C_{20}, 12.4; C_{22}, 14.6; and C_{24}, 17.0; these were used to calculate respective C values of fatty acid products.

RvD1 Preparation—RvD1 was prepared using a one-pot reaction by incubating DHA and soybean LOX (type IV; from Sigma) as in previous studies (5, 17). Briefly, DHA (2 mg) was incubated with soybean LOX (100 kilounits, 701 kilounits/mg of protein, 3.6 mg of protein/ml), in borate buffer (5 ml, pH 9.3) at 4 °C. The substrate DHA in micelle suspensions was vortexed (~15 min, at room temperature), and the isolated soybean LOX (100 kilounits) was added to the micelle suspensions at 15- and 30-min intervals. These incubations were terminated at 40 min with addition of cold methanol (20 ml) followed by addition of $NaBH_4$ for reduction. Next, they were taken for extraction using C18 solid phase (20) and subsequent analyses. The product isolated by RP-HPLC matched RvD1 produced by isolated human PMN (5).

Total Organic Synthesis—Both RvD1 and AT-RvD1 were synthesized from chiral starting materials of known chirality in enantiomerically and geometrically pure form via total organic synthesis, which will be reported separately.[3] The structures of synthetic RvD1 and AT-RvD1 methyl esters were characterized by NMR spectroscopy.

Methanol Trapping with Human PMNs—Human whole (venous) blood was collected with heparin from healthy volunteers that declined taking medication for 2 weeks prior to donation, according to Brigham and Women's Hospital protocol 88-02642. Briefly, PMNs were freshly isolated from whole blood by Ficoll gradient and enumerated. 17*S*-hydro(peroxy)-DHA (3 μg) was incubated with human PMN suspensions (30–50 × 10^6 cells/ml) and zymosan A (100 μg/ml) in Dulbecco's phosphate-buffered saline (with Mg^{2+} and Ca^{2+}) at 37 °C for 5 min (5). Acidified MeOH (apparent pH ~ 3 after mixing, 4 °C) was added, and the mixture was incubated at 4 °C for 10 min. The samples were rapidly neutralized and taken for C18 solid phase extraction and analyses.

Endothelial Cell Isolation and Culture—Human microvascular endothelial cells (HMEC-1) were a gift of Francisco Candal,

[3] N. A. Petasis, J. Uddin, and C. N. Serhan, manuscript in preparation.

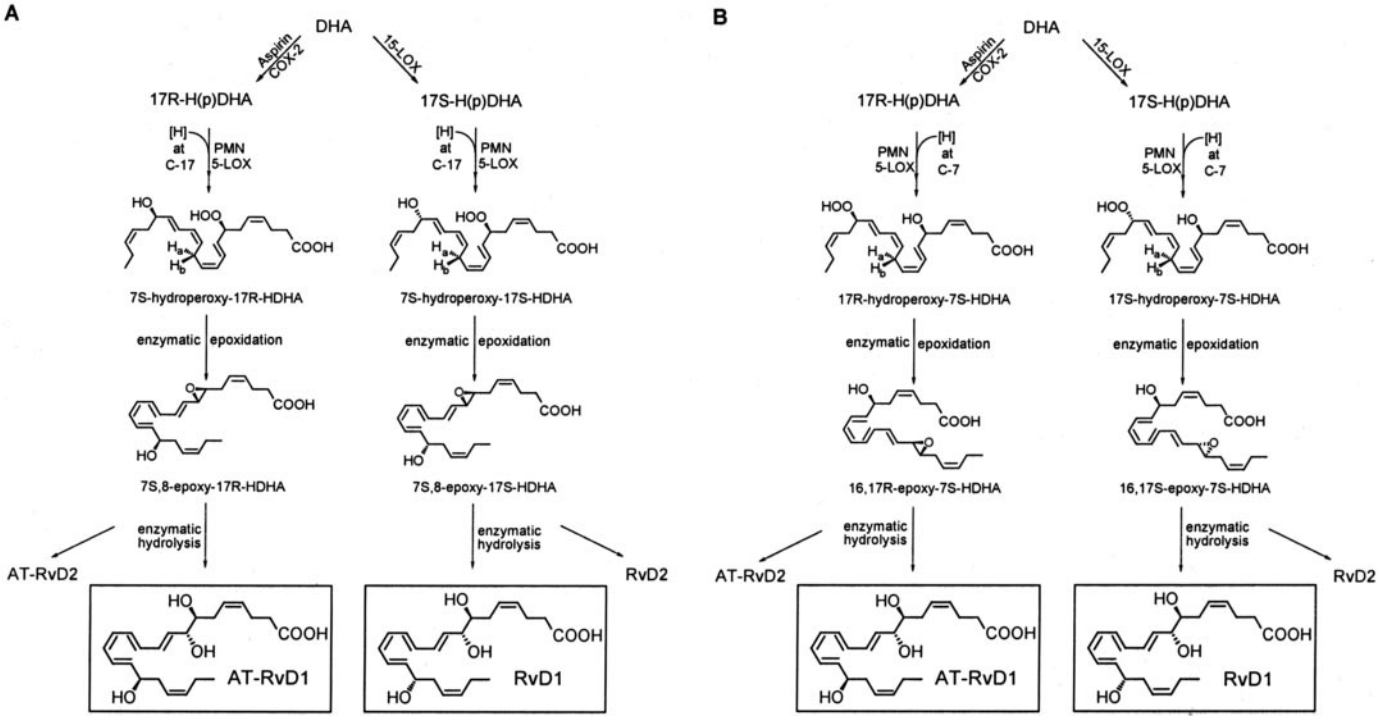

FIGURE 1. **RvD1 and AT-RvD1 biosynthesis.** *A*, pathways proposed for RvD1 and AT-RvD1. RvD1 and AT-RvD1 are both generated from DHA. 15-LOX converts DHA into 17*S*-H(p)DHA (15), whereas aspirin-acetylated cyclooxygenase-2 generates predominately *R*-containing 17*R*-H(p)DHA (5). The 17-hydro(peroxy) products of DHA are then each converted rapidly by 5-LOX in PMNs into 7,8-epoxide-containing intermediates. Enzymatic hydrolysis of each 7,8-epoxide intermediate follows to form the bioactive RvD1 and AT-RvD1. *B*, additional pathway for RvD1 and AT-RvD1. DHA is converted to 17*R/S*-hydro(peroxy)-DHA by either aspirin-acetylated cyclooxygenase-2 (17*R*-H(p)DHA) or 15-LOX (17*S*-H(p)DHA) as in Fig. 1*A*. The 17-hydro(peroxy) product is then oxygenated at the 7 position by 5-LOX to 7*S*-hydro(peroxy), 17-H(p)DHA, which is then converted in theory to a 16,17-epoxide-containing DHA intermediate. This 16(17)-epoxide, if produced, could then be opened via hydrolytic 1,10 addition to yield either RvD1, AT-RvD1, or their respective *trans* isomers (see text for details).

Centers for Disease Control, Atlanta, GA (23) and were cultured by a modification of methods described previously (24, 25). In brief, HMEC-1 were harvested with 0.1% trypsin and incubated at 37 °C in 95% air/5% CO_2. Culture medium was supplemented with heat-inactivated fetal bovine serum, penicillin, streptomycin, L-glutamine, epidermal growth factor, and hydrocortisone. For preparation of experimental monolayers, confluent endothelial cells were seeded at $\approx 10^5$ cells/cm^2 onto permeable polycarbonate inserts.

Human PMNs and Transmigration—PMNs for transmigration were isolated as above with acid citrate dextrose as the anticoagulant as described with minor modification (26). Double density gradients of Histopaque 1077 and 1119 (Sigma) were prepared, and whole venous blood was applied to each gradient and centrifuged at 700 × *g* for 30 min at room temperature. PMNs localized to the buffy coat directly above the red blood cells were removed. Residual red blood cells were removed by lysis in ice-cold NH_4Cl buffer. PMNs were >90% as determined by microscopic evaluation and suspended 1×10^8 cells/ml in $HBSS^-$ (with 10 mM Hepes, pH 7.4, and without Ca^{2+} or Mg^{2+}, Sigma-Aldrich). PMNs were used within 2 h of isolation.

PMNs were incubated with 0–1000 nM RvD1 or AT-RvD1 in $HBSS^-$ at room temperature for 15 min. Migration assays were performed (27). Briefly, 10^6 PMNs were added to the upper chambers of Transwell inserts plated with HMECs. A chemotactic gradient was established by adding $HBSS^+$ to the upper and 100 nM *n*-formylmethionylleucylphenylalanine (fMLP) in $HBSS^+$ to the lower chambers. PMN transmigration was carried out at 37 °C for 30 min, after which transmigrated PMNs were quantified by monitoring myeloperoxidase (MPO) (27).

Acute Inflammation—Murine peritonitis was performed (28) using 6- to 8-week-old FVB male mice (Charles River Laboratories, Wilmington, MA) that were fed laboratory Rodent Diet 5001 (Purina Mills, Richmond, IN). After anesthetization with isoflurane, compounds were administered in 100 μl of phosphate-buffered saline intravenously through a tail vein. Zymosan A (1 mg/1 ml in sterile saline, Sigma) was injected intraperitoneally immediately following compound administration. In accordance with the Harvard Medical Area Standing Committee on Animals protocol 02570, mice were sacrificed after 4 h and peritoneal lavages were rapidly collected in Dulbecco's phosphate-buffered saline (minus Mg^{2+} and Ca^{2+}, 5 ml). Aliquots of the lavage were stained with trypan blue and enumerated by light microscopy. For differential leukocyte counts, 100 μl of the lavage was added to 300 μl of 15% bovine serum albumin and centrifuged onto microscope slides at 1600 rpm for 4 min using a Cytofuge (StatSpin, Norwood, MA). The slides were allowed to air dry, and cells were visualized using a modified Wright-Giemsa stain (Sigma).

Recombinant Enzymes—Activity of 15-prostaglandin dehydrogenase/eicosanoid oxidoreductase (denoted here and throughout as EOR as in Ref. 29) was monitored spectrophotometrically by the formation of NADH from NAD^+ at 340 nm. Substrates in ethanol were dried down under N_2 stream and resuspended in buffer containing Tris-HCl (0.1 M, pH 9.0,

Sigma) and NAD^+ (1.0 mM, Sigma) to a final concentration of 20 μM (100-μl total volume). Reactions were initiated with the addition of partially purified EOR (0.05 μg/incubation), and absorptions were read every 30 s for 25 min at 37 °C.

Oxo-RvD1 Products—RvD1-ME or RvD1 (10 μg) was dried down under N_2 stream and suspended in buffer containing Tris-HCl (100 μl, 0.1 M, pH 7.4, Sigma) and NAD+ (1.0 mM, Sigma). Enzymatic conversion was initiated by the addition of partially purified EOR (5 μg) and allowed to proceed for 2 h at 37 °C. After 2 h, these reactions were stopped with 2 volumes of cold methanol, and samples were extracted with C18 solid phase extraction.

RESULTS

Comparison of Synthetic RvD1 and AT-RvD1—To assign the complete stereochemistry of natural RvD1 and determine whether RvD1 and its aspirin-triggered form AT-RvD1 (Fig. 1) share biological properties, as well as match their reported properties and actions (5, 15), it was essential to first establish the spectroscopic and physical properties of the synthetic materials (Fig. 2). The structure and stereochemistry of synthetic RvD1 and AT-RvD1 were unambiguous on the basis of their total synthesis from chiral-starting materials of known stereochemistry. The *R/S* configurations of C-7, C-8, and C-17 were directly derived from starting materials of the same chirality. For example, the C-17 *R* alcohol chirality was retained from the starting material (*S*)-(−)-glycidol and the C-17*S* retained from (*R*)-(+)-glycidol. The *Z/E* configuration of the double bonds was determined and confirmed using ^1H NMR (COSY). Both RvD1 and AT-RvD1 gave very similar spectra (Fig. 2), yet displayed different chromatographic behaviors with RP-HPLC (Fig. 3).

Liquid chromatography analysis gave UV chromatograms when monitored at 301 nm with major peak AT-RvD1 at 13.9 min separating and eluting before RvD1 at 15.1 min (Fig. 3*A*). The column and mobile phase parameters used here permitted separation of these two diastereomers by ~1.2 min. The carboxyl-methyl esters of RvD1 and AT-RvD1 also resolved using essentially identical conditions (not shown). Further analysis of both RvD1 and AT-RvD1 demonstrated the major anion for both MS spectra was at *m/z* 375 (see Fig. 3, *B* and *C*, cleavage site *a*), which represents [M-H] for both RvD1 and AT-RvD1. These were consistent with the original mass spectra and structural elucidation of these resolvins produced *in vivo* in mouse exudates and with isolated human leukocytes (5).

As expected, analysis of the MS/MS spectrum obtained for both RvD1 and AT-RvD1 gave essentially the same fragmentation patterns (Fig. 3). Prominent daughter ions were obtained for both compounds at *m/z* 357 [*a*-H_2O]; 339 [*a*-2H_2O]; 331 [375-CO_2] (see Fig. 3, *B* and *C*, cleavage site *b*); 321 [*a*-3H_2O]; 313 [*b*-H_2O]; 295 [*b*-2H_2O]; 277 [375-CHO-CH_2-$(CH)_2$-CH_2-CH_3] (see Fig. 3, *B* and *C*, cleavage site *d*); 259 [*d*-H_2O]; 241 [*d*-2H_2O]; 233 [375-CHOH-CH_2-$(CH)_2$-$(CH2)_2$-CO_2] (see cleavage site *c*); 215 [*c*-H_2O]; 141 [CHO-CH_2-$(CH)_2$-$(CH2)_2$-COO^-] (see cleavage site *c′*) essentially matching the ions reported earlier for endogenous RvD1 and AT-RvD1 isolated from murine inflammatory exudates and human PMN (Fig. 3*D* and *cf.* Ref. 5).

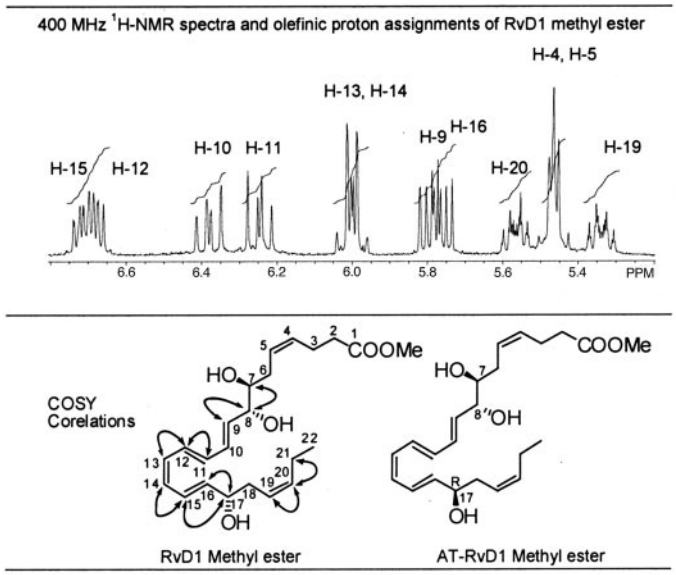

Position	δ (mult, *J*/Hz)	δ (mult, *J*/Hz)
Olefinic H		
H-4, H-5	5.45 (m)	5.46 (m)
H-9	5.78 (dd, *J* = 14.8, 6.8)	5.79 (dd, *J* = 15.2, 7.2)
H-10	6.36 (dd, *J* = 14.8, 10.8)	6.38 (dd, *J* = 14.8, 10.8)
H-11	6.24 (dd, *J* = 14.8, 10.8)	6.25 (dd, *J* = 14.8, 10.8)
H-12	6.67 (dd, *J* = 14.8, 10.4)	6.68 (dd, *J* = 14.8, 10.4)
H-13, H-14	5.99 (dd, *J* = 10.4, 6.8)	6.00 (dd, *J* = 10.4, 6.8)
H-15	6.71 (dd, *J* = 14.8, 10.8)	6.70 (dd, *J* = 14.8, 10.4)
H-16	5.75 (dd, *J* = 14.8, 8.6)	5.76 (dd, *J* = 15.2, 6.0)
H-19	5.33 (qt, *J* = 10.4, 1.6)	5.31 (qt, *J* = 10.8, 1.2)
H-20	5.56 (qt, *J* = 10.4, 1.6)	5.57 (qt, *J* = 10.8, 1.0)
Other H		
H-2, H-3, H-6, H-18	2.41-2.16 (m)	2.42-2.15 (m)
H-7	3.71 (m)	3.69 (m)
H-8, H-17	4.21 (m)	4.22 (m)
H-21	2.06 (m)	2.07 (m)
H-22	0.96 (t, *J* = 7.6)	0.95 (t, *J* = 7.6)
-OMe	3.63 (s)	3.64 (s)

FIGURE 2. **Physical and spectroscopic properties of RvD1 and AT-RvD1.** 400-MHz ^1H NMR spectra and assignments of RvD1 methyl ester olefinic protons as well as AT-RvD1 methyl ester in $CDCl_3$ prepared by total organic synthesis. The NMR spectrum of the olefinic region of RvD1 methyl ester is shown. Assignments were made on the basis of COSY correlations (shown).

Of interest, as observed in the comparison of LXA_4 and its endogenous aspirin-triggered form 15-epi-LXA_4 (30), successive MS/MS analysis gave subtle differences in the intensity of several of the main daughter ions between RvD1 and its 17 epimer, AT-RvD1. Table 1 reports a summary of the prominent ions (both LC-MS/MS and GC-MS) and chromatographic properties of synthetic RvD1 and AT-RvD1 using parameters obtained originally for the endogenous resolvins (5, 15, 31). The present results with both synthetic and endogenous RvD1 confirm the original assignments of its basic structure (Table 1).

Matching of Enzymatically Generated RvD1 with Synthetic RvD1—Having established the physical properties of synthetic RvD1, we next sought evidence to determine whether it was identical to the biologically active enzymatically generated material as well as assign the geometry of its conjugated double

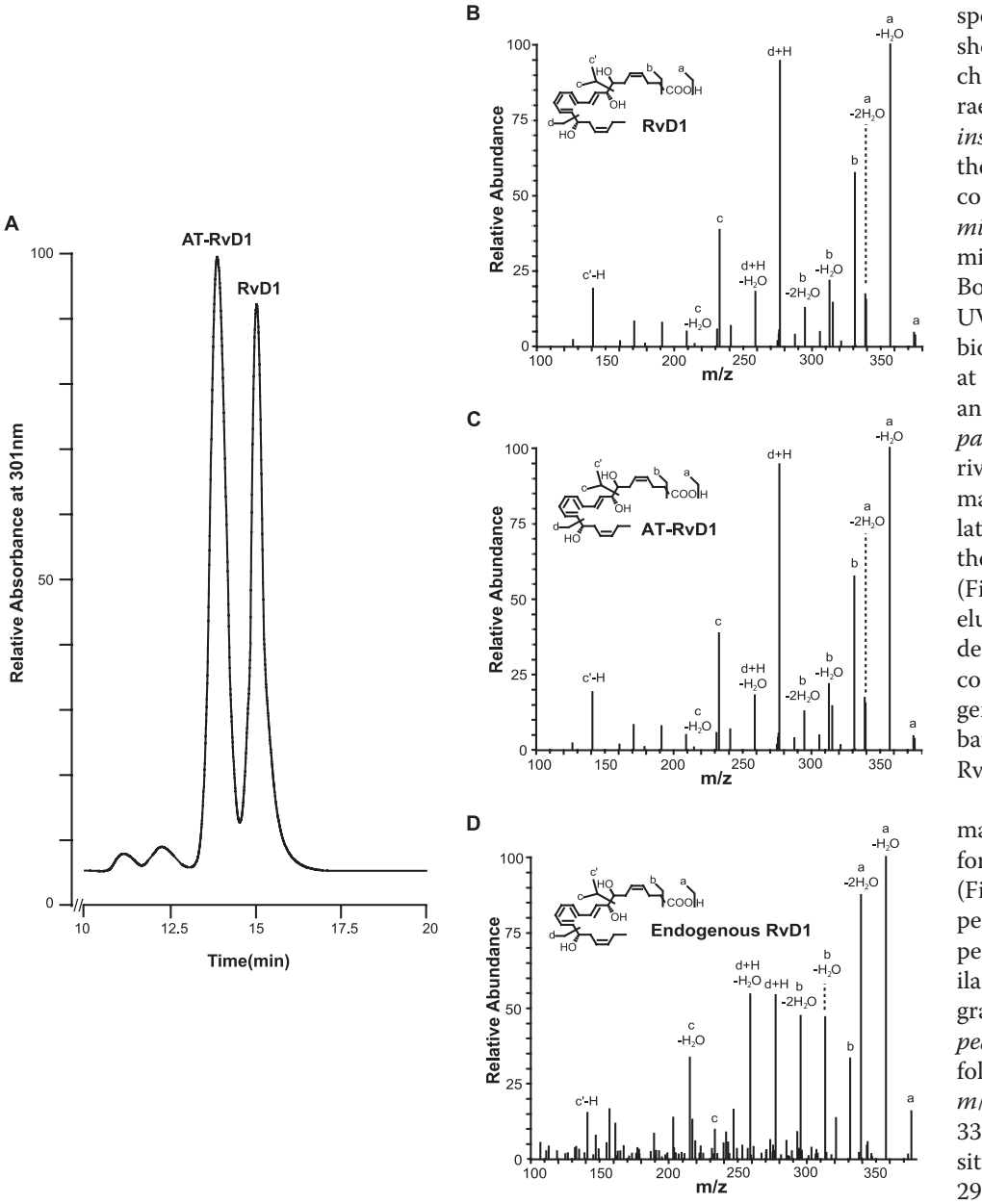

FIGURE 3. **Physical properties of RvD1 and AT-RvD1.** *A*, LC chromatograms plotted at UV absorbance 301 nm. RvD1 and AT-RvD1 separate in this HPLC system with retention times of 15.1 and 13.9 min. *B* and *C*, MS/MS analysis of RvD1 at $m/z = 375$. *D*, MS/MS analysis of AT-RvD1 at $m/z = 375$. See "Experimental Procedures" for details.

bonds and chirality of the alcohol group at the carbon 8 position that remained to be established (5, 15). It was essential to take this approach, because the nanogram amounts obtained from human cells and inflammatory exudates permitted assigning the basic structure and bioactions of RvD1 but precluded direct determination of the complete stereochemistry of the biologically derived RvD1 (5). To this end, biogenic RvD1 was prepared by incubating DHA with isolated 15-LOX type I (*i.e.* soybean LOX type IV, see "Experimental Procedures") using a one-pot incubation procedure that employed micellar substrate presentation (15, 17). Liquid chromatographic analysis of this material resulted in one major component at 7.5 min monitored at 301 nm (Fig. 4*A*) and two minor ones at 6.1 and 6.5 min (Fig. 4*A*, *top panel*). Each of these three components exhibited a triplet UV spectrum with λ_{max} at 301 nm with shoulders at 289 nm and 315 nm, characteristic of a conjugated tetraene system (Fig. 4*A*, *top panel inset*). Similar analysis with the synthetic material resulted in a major component at 7.6 min (see Fig. 4*A*, *middle panel*) and a minor at 6.6 min when monitored at 301 nm. Both of these also demonstrated a UV spectrum identical to that of the biogenic/enzymatic material: λ_{max} at 301 nm with shoulders at 289 nm and 315 nm (see Fig. 3*A*, *middle panel inset*). Human leukocyte-derived RvD1 co-eluted with the major product, obtained with isolated LOX, and further analysis of the biogenic and synthetic mixtures (Fig. 4*A*, *lower panel*) resulted in co-elution at 7.5 min. These results demonstrate that the predominant component of the RvD1 mixture generated by the isolated LOX incubations also matched synthetic RvD1 (Fig. 4).

LC-MS/MS analysis of the enzymatically generated RvD1 was performed and monitored at $m/z = 375$ (Fig. 4*B*) and resulted in one major peak at 12.4 min and two minor peaks at 11.0 min and 9.5 min, similar to the RP-HPLC chromatograms in Fig. 4*A*. MS/MS analysis of *peak I* (Fig. 4*C*) demonstrated the following prominent daughter ions: m/z 357 [a-H_2O]; 339 [a-$2H_2O$]; 331 [375-CO_2] (see Fig. 3*C*, cleavage site *b*); 321 [a-$3H_2O$]; 313 [b-H_2O]; 295 [b-$2H_2O$]; 277 [375-CHO-CH_2-$(CH)_2$-CH_2-CH_3] (see Fig. 3*C*, cleavage site *d*); 259 [d-H_2O]; 241 [d-$2H_2O$]; 233 [375-CHOH-CH_2-$(CH)_2$-$(CH2)_2$-CO_2] (cleavage site *c*); 215 [c-H_2O]; and 141 [CHOH-CH_2-$(CH)_2$-$(CH2)_2$-COO^-] (cleavage site *c'*). The fragmentation pattern of this enzymatically generated RvD1 matched that of the RvD1 prepared by total organic synthesis (Fig. 3*B*).

To obtain further evidence for matching, GC-MS analysis was performed as in the original identification and basic structural elucidation of the resolvins (5). Fig. 4*D* reports and illustrates a representative mass spectrum and prominent ions obtained with enzymatically generated RvD1 that was treated with diazomethane and subsequently converted to its corresponding trimethylsilyl derivative and subject to GC-MS. This spectrum (Fig. 4*D*) demonstrates the following major ions: m/z 537 [606-CH_3-CH_2-$(CH)_2$-CH_2] (cleavage site *e*); 479 [606-CH_2-$(CH)_2$-$(CH_2)_2$-$COOCH_3$] (see Fig. 4*D*, cleavage site *a*);

TABLE 1
Physical and chemical properties by HPLC, LC-MS/MS, and GC-MS analyses

	RP-HPLC Retention Time	LC/MS Major Ions*	GC/MS Major Ions*	C Value ‡	UV Absorbance Spectra*
RvD1 7S, 8R, 17S trihydroxy-4Z, 9E, 11E, 13Z, 15E, 19Z-DHA 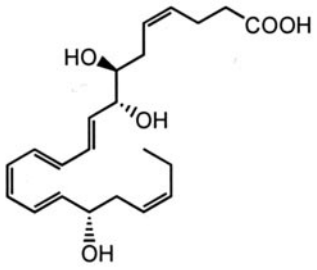	15.1 min	375, 331, 277, 259, 233, 141	606, 537, 479, 435, 377, 331, 229, 171	25.9 ± 0.2	301 nm (shoulders at 289 nm and 316 nm)
AT-RvD1 7S, 8R, 17R trihydroxy-4Z, 9E, 11E, 13Z, 15E, 19Z-DHA 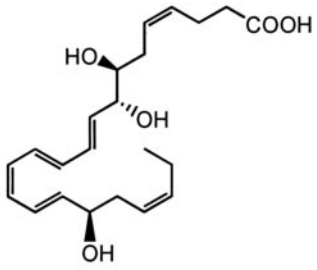	13.9 min	375, 331, 277, 259, 233, 141	606, 537, 479, 435, 377, 331, 229, 171	26.3 ± 0.2	301 nm (shoulders at 289 nm and 316 nm)

* See "Experimental Procedures" for further details.

435 [606-CH_3-CH_2-$(CH)_2$-CH_2-CHOSi$(Me)_3$] (cleavage site *d*); 377 [606-CHOSi$(Me)_3$-CH_2-$(CH)_2$-$(CH_2)_2$-$COOCH_3$] (cleavage site *b′*); 331 [CHOSi$(Me)_3$-CHOSi$(Me)_3$-CH_2-$(CH)_2$-$(CH_2)_2$-$COOCH_3{}^+$] (cleavage site *c*); 229 [CHOSi$(Me)_3$-CH_2-$(CH)_2$-$(CH_2)_2$-$COOCH_3$] (cleavage site *b*); and 171 [CH_3-CH_2-$(CH)_2$-CH_2-CHOSi$(Me)_3$] (cleavage site *d′*). Based on retention time, the C-value was determined to be 25.9 ± 0.2 (see "Experimental Procedures"). This fragmentation pattern, UV spectrum, and C-value are consistent with those obtained for GC-MS analysis of biogenic RvD1 and those prepared by total organic synthesis (see Table 1).

RvD1 Biosynthesis Proceeds via an Epoxide-containing Intermediate—RvD1 is generated *in situ* from DHA by two sequential oxygenations at the carbon 7 and 17 positions incorporating molecular oxygen predominately in the *S* configuration in both positions (5). The third alcohol group at position 8 is proposed to be generated via enzymatic opening of an epoxide-containing intermediate (see Fig. 1). Given the conjugated double bond system generated when C7 and C17 are oxygenated, RvD1 could theoretically be generated by either a 1,10 addition into the conjugated system involving a possible 16,17-epoxide-containing intermediate from DHA or via an enzyme-directed hydrolysis of a 7,8-epoxide intermediate (see "*Proposed Pathways*" and "*Additional Pathway*" in Fig. 1, *A* and *B*). In addition to the soybean LOX-mediated generation of RvD1 utilized in Fig. 3, RvD1 can also be generated by incubating 17-H(p)DHA with activated human PMNs (15). Because this two-step biosynthesis is thought to occur *in vivo* via cell-cell interactions within resolving inflammatory exudates (5), evidence was sought to establish the role of an epoxide intermediate in RvD1 biosynthesis and determine which routes predominate in the biosynthesis. To this end, 17*S*-hydrox(peroxy)-DHA was incubated with human PMNs, followed by incubation with acidic methanol to trap epoxide intermediates. LC-MS/MS analysis of the trapping products obtained from these incubations revealed two major components (see Fig. 5, *peaks Ia* and *Ib*) when monitored at m/z = 389, the M-H for methoxy-trapping products. MS/MS analysis of *peak Ia* identified it as methoxy-RvD1 trapping products by the presence of the following prominent daughter ions: m/z 374 [*a*-CH_3], 371 [*a*-H_2O]; 357 [*a*-MeOH]; 345 [389-CO_2]; 339 [*a*-MeOH-H_2O]; 302 [320-H_2O]; 275 [290-CH_3]; 257 [275-H_2O]; and 231 [275-CO_2]. The presence of these ions is consistent with the formation of a methoxy-containing trapping product formed from an

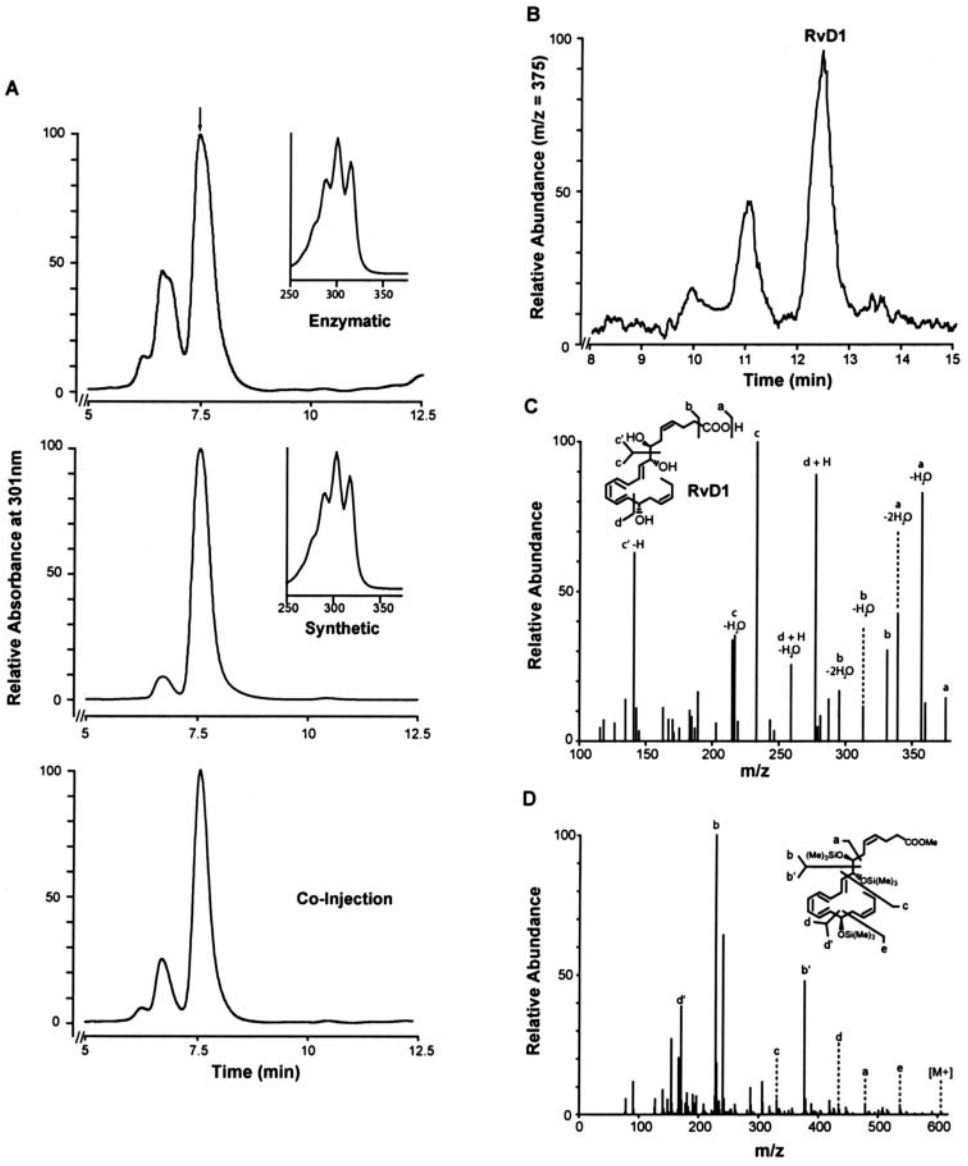

FIGURE 4. **Comparison of RvD1 obtained via LOX-catalyzed synthesis *versus* total organic synthesis.** In *A*: *Top panel*, LC chromatogram of enzymatically produced RvD1. The *inset* represents a UV spectrum of compound I (retention time = 7.5 min). *Middle panel*, LC chromatogram of synthetic RvD1. The *inset* represents a UV spectrum of compound I (retention time = 7.5 min). *Lower panel*, LC chromatogram obtained from co-injection of enzymatic and synthetic RvD1 mixture. *B*, LC-MS/MS profile of enzymatically produced RvD1 obtained for *m/z* 375. *C*, MS/MS analysis of LOX-produced RvD1 at *m/z* = 375. *D*, GC-MS spectrum of the derivatized product obtained with enzymatically produced RvD1. MS was obtained following treatment with diazomethane and trimethylsilane. See "Experimental Procedures" for further details.

epoxide-containing intermediate derived from the 17*S*-H(p)DHA precursor in human PMNs. The material in *Ib* gave essentially the same prominent ions obtained for *Ia* in Fig. 5. The identification of these ions in MS/MS from both trapping products *Ia* and *Ib* establishes the role of an epoxide intermediate; both were consistent with a 7*S*-hydroxy-8-methoxy-containing trapping product as well as a 7*S*-hydroxy-16-methoxy-containing trapping product. Specific ions in *Ia* and *Ib* were not evident to distinguish and support a preference in the formation of 8-methoxy- *versus* a 16-methoxy-containing trapping product generated from a 7*S*,8*S*-epoxy-17*S*-HDHA intermediate. Hence, it is likely that a carbonium cation is generated in the H^+ and MeOH trapping conditions that gives both 16-methoxy and 8-methoxy trapping products as illustrated in Fig. 5. It is noteworthy that 17*S*-HDHA gave similar trapping products with activated human PMN but in lower amounts than with 17*S*-H(p)DHA as substrate, and the isolated 15-LOX also gave the methoxy-trapping products (not shown). Hence, identification of these methoxy-trapping products (both 8-methoxy- and 16-methoxy-containing) provides direct evidence for the formation of an epoxide intermediate in the biosynthesis of RvD1.

Anti-inflammatory Actions of RvD1 and AT-RvD1—Next, we compared the actions of RvD1 and AT-RvD1 on human PMN transendothelial migration, the first event in acute inflammation (2, 3, 5). For these experiments, PMNs were exposed to either RvD1 or AT-RvD1 (0–1000 nM) to assess their impact with fMLP-stimulated (100 nM) transendothelial migration. As shown in Fig. 6*A*, both RvD1 and AT-RvD1 stopped PMN transmigration in a concentration-dependent fashion ($p < 0.01$ for both AT-RvD1 and RvD1). Although both molecules potently reduced PMN transmigration by as much as 65 ± 8% at 1 μM concentrations of AT-RvD1 ($EC_{50} \sim 30$ nM), no statistically significant differences were noted between RvD1 or its aspirin-triggered form AT-RvD1 at the concentrations tested (p = not significant by analysis of variance). A reduction in PMN transmigration of ~50% was obtained with concentrations as low as 10 nM.

Earlier results demonstrated that both 17*S* and 17*R* D series resolvins (RvD1 and AT-RvD1, respectively) significantly reduce PMN infiltration *in vivo* as effectively as equivalent doses of indomethacin (15). Because of the presence of additional resolvins within the preparations of isolated RvD1 and AT-RvD1 series (5, 15), the relative potencies of RvD1 remained to be established *in vivo*. Using purified synthetic RvD1 and AT-RvD1, we determined their potency and assessed whether they were indeed anti-inflammatory *in vivo*. Both RvD1 and AT-RvD1 limited total leukocytic infiltration (Fig. 6*B*) at each dose tested with the maximal decrease in total leukocytes with as little as a 100 ng dose per mouse. At the 10-ng dose, AT-RvD1 reduced leukocytic infiltration to a greater extent than RvD1 (~23% and ~8–10%, respectively; $p < 0.05$, two-tailed Student's t test).

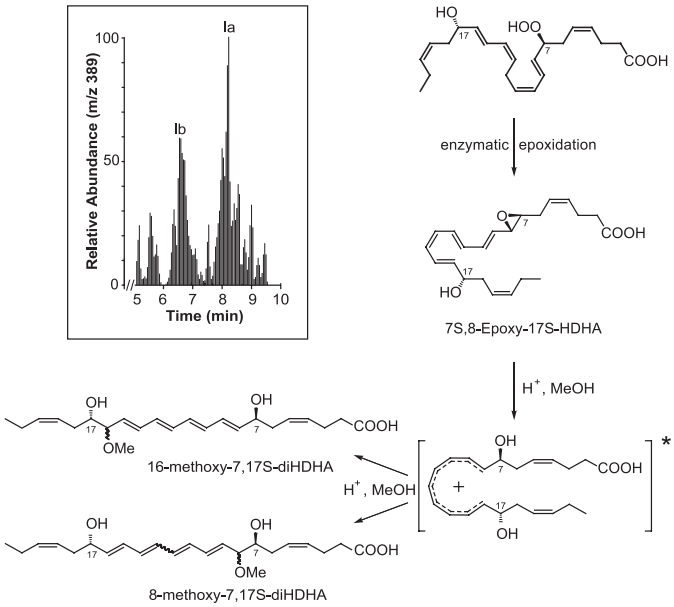

FIGURE 5. **Trapping epoxide intermediate in the biosynthesis of RvD1.** Proposed 7,8-epoxide intermediate and carbonium cation involved in the formation of epoxide-derived trapping products in acid MeOH. PMNs ($30-50 \times 10^6$) were incubated with 17*S*-hydro(peroxy)-DHA (3 μg) and zymosan A (100 μg/ml). Incubations were then stopped with acidic methanol, and trapping products obtained were extracted and taken for LC-MS/MS analyses. *Left inset*: LC-MS chromatogram obtained from selective ion monitoring at m/z = 389 yielded two methoxy products (*Ia* and *Ib*). See "Experimental Procedures" for further details.

Both RvD1 and AT-RvD1 exhibited a dose-dependent reduction in PMN infiltration (Fig. 6*B*) with similar potency and efficacy (maximal inhibition of ~35% at dose of 100 ng/mouse). Furthermore, both compounds were bioactive at the lowest dose administered (1 ng/mouse), demonstrating the very potent actions of these mediators.

Conversion and Inactivation of RvD1 and AT-RvD1—D series resolvins are generated and act locally at sites of inflammation (15, 31), much like their arachidonic acid-derived cousins, LXs. LXs are rapidly inactivated by EORs (29, 32). Along these lines, further enzymatic conversion of the D series resolvins remained of interest. Therefore, we sought to determine whether RvD1 and AT-RvD1 were substrates for the EOR-initiated further metabolism. To this end, RvD1, AT-RvD1, or, for purposes of direct comparison, LXA_4 (~20 μM) was incubated with EOR (0.05 μg), and the reactions were monitored by the formation of NADH, an essential cofactor for the enzyme (Fig. 7). Although LXA_4 was converted most readily, RvD1 was converted to a similar extent within 25 min in these incubations. The kinetics for conversion, however, were slower for RvD1 than LXA_4 as can be seen by the statistically significant difference in NADH formation at 5 min (~10 μM NADH formation *versus* ~6 μM NADH formation with LXA_4 and RvD1 as substrates, respectively; $p < 0.05$, two-tailed Student's *t* test). Interestingly, AT-RvD1, which differs from RvD1 only in the configuration of the 17-hydroxyl group, namely 17*R* for AT-RvD1, was essentially resistant to rapid conversion.

Because RvD1 was converted by the EOR, we determined the structure and bioactions of the metabolite(s). Using RP-HPLC analysis, the UV absorbance spectra of RvD1-ME and the metabolites were measured (Fig. 8, *A* and *B*). The presence of a conjugated tetraene within RvD1 is responsible for its characteristic triplet chromophore with a λ_{max} of 301 nm. LC analysis of the metabolites yielded two distinct products that eluted at 15.9 and 17.6 min, both containing a single broad UV absorbance at λ_{max} = 351 nm (Fig. 8*B*). Because the EOR utilized, *i.e.* 15-prostaglandin dehydrogenase, oxidizes alcohols to their respective ketones as in the inactivation of prostaglandin E_2 (reviewed in Ref. 33) and LXA_4 (29), the potential single oxo-containing products generated might be 7-oxo-RvD1, 8-oxo-RvD1, or 17-oxo-RvD1. Formation of a 7-oxo product from RvD1 would retain the same conjugated tetraene structure; the absence of this chromophore indicated that 7-oxo-RvD1 is not likely to be generated by this EOR. Both 8-oxo- and 17-oxo-RvD1 would extend the conjugation of the tetraene system to the corresponding carbonyl group, thereby lowering the difference in energy (ΔE) between the ground and excited electronic states. Lowering the ΔE results in a red-shift of the absorption maximum analogous to the shift in 15-oxo-LXA_4 (29). Therefore, the presence of the red-shifted UV absorbance for compounds I and II suggests that the two main metabolites were 8-oxo-RvD1 and 17-oxo-RvD1.

To confirm the identity, compounds I and II and RvD1 were isolated using these conditions and subjected to LC-MS/MS analyses. Monitoring at m/z = 373 yielded two main peaks with retention times of 9.9 and 10.9 min, respectively (Fig. 8*C*). MS/MS analysis of peak I identified it as the 8-oxo-RvD1 by the presence of the following prominent daughter ions: m/z 355 [*a*-H_2O]; 329 [373-CO_2] (see Fig. 8*D*, cleavage site *b*); 311 [*b*-H_2O]; 293 [*b*-2H_2O]; 275 [373-CHO-CH_2-$(CH)_2$-CH_2-CH_3] (Fig. 8*D*, cleavage site *e*); 261 [373-CH_2-$(CH)_2$-$(CH2)_2$-CO_2] (cleavage site *c*); 243 [*c*-H_2O]; and 141 [CHO-CH_2-$(CH)_2$-$(CH2)_2$-COO^-] (cleavage site *d*). MS/MS analysis of compound II demonstrated that it is 17-oxo-RvD1 by the presence of the following prominent daughter ions: m/z 355 [*a*-H_2O]; m/z 337 [*a*-2H_2O]; 329 [373-CO_2] (see Fig. 8*E*, cleavage site *b*); 311 [*b*-H_2O]; 293 [*b*-2H_2O]; 275 [373-CHO-CH_2-$(CH)_2$-CH_2-CH_3] (cleavage site *d*); 231 [373-CHOH-CH_2-$(CH)_2$-$(CH2)_2$-CO_2] (cleavage site *c*); and 213 [*c*-H_2O]. 17-Oxo-RvD1 was also produced from RvD1 in murine lung and identified using the same criteria and prominent ions in its MS/MS spectrum (Fig. 9).

Having identified these further metabolic products of RvD1, we next determined whether 8-oxo-RvD1 and 17-oxo-RvD1 also displayed the *in vivo* anti-inflammatory actions characteristic of their precursor RvD1. As shown in Fig. 10, 8-oxo-RvD1 (10 ng/mouse) limited PMN infiltration in murine peritonitis by a statistically significant 41% ($p < 0.05$, two-tailed unpaired Student's *t* test), which was comparable to RvD1 (44%, $p < 0.05$, two-tailed unpaired Student's *t* test) (Fig. 10). In sharp contrast, 17-oxo-RvD1 did not decrease PMN infiltration *in vivo* in a statistically significant manner. When compared with the actions of RvD1, 8-oxo-RvD1 was as effective (~93% the activity of RvD1), whereas 17-oxo-RvD1 was significantly less bioactive (~10%, $p < 0.05$, two-tailed unpaired Student's *t* test). Together these results indicate that 17-oxo-RvD1 is the inactivation product of RvD1.

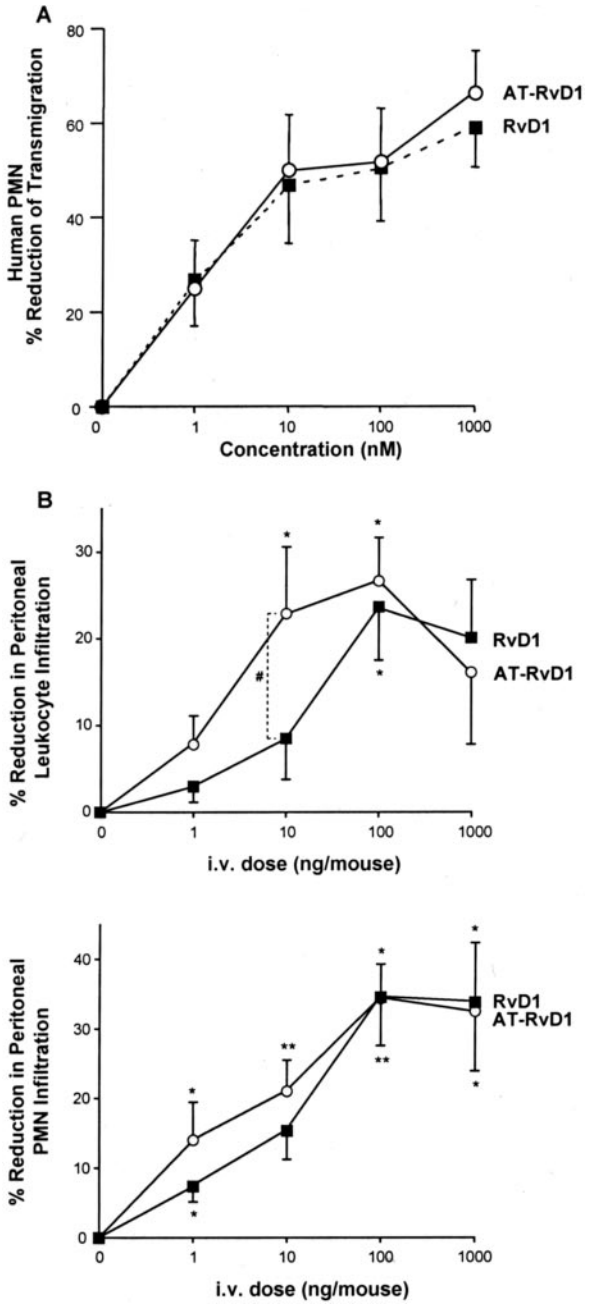

FIGURE 6. **Potent anti-inflammatory actions of RvD1; comparison with AT-RvD1.** *A*, human PMN transendothelial migration. Freshly isolated PMNs were incubated with either 0–1000 nM RvD1 or AT-RvD1 for 15 min prior to exposure to endothelial monolayers. PMNs were applied to HMEC inserts and allowed to migrate across an fMLP chemotactic gradient. After 30 min the number of migrated cells was quantified by MPO. Results were normalized to migration of untreated PMN as control and expressed as percentage reduction. *B*, dose-dependent reduction of acute inflammation by RvD1 and AT-RvD1 in murine peritonitis. RvD1 (■) or AT-RvD1 (○) was injected by intravenous bolus injection (0.05, 0.5, 5.0, or 50 μg kg^{-1} in 100 μl of sterile saline) via the tail vein of 6- to 8-week-old male FVB mice followed by peritoneal injection of zymosan A (1 mg/ml). Resolvins were tested *in vivo* as their carboxymethyl esters. Peritoneal lavages were collected (4 h), and total leukocytes, PMNs, and monocytes were enumerated. Reduction of total leukocyte and PMN infiltration was determined by comparison to vehicle control (100 μl of sterile saline). In *B*: *Upper panel*, dose-dependent comparison between RvD1 (■) and AT-RvD1 (○) actions on total leukocytic infiltration. *Lower panel*, dose-dependent comparison between RvD1 (■) and AT-RvD1 (○) actions on PMN infiltration. Values represent mean ± S.E., $n = 3, d \geq 2$; *, $p < 0.05$; **, $p < 0.005$ when compared with vehicle with zymosan (as control); #, $p < 0.05$ when compared between RvD1 and AT-RvD1.

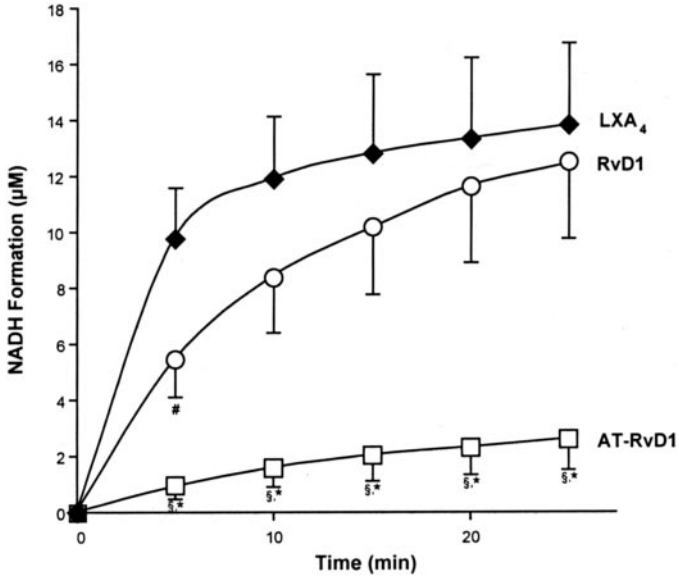

FIGURE 7. **Conversion of RvD1 and AT-RvD1 by rEOR.** LXA_4, RvD1, or AT-RvD1 (~20 μM) were each incubated with 50 ng of EOR. Incubations were performed at 37 °C (0.1 M Tris-HCl, pH 9.0, 1 mM NAD^+, 100 μl of total volume) for 25 min, and the rate of NADH formation was monitored. Initial reaction velocities were calculated using linear regression analysis. ◆, LXA_4; ○, RvD1; and □, AT-RvD1. Values represent the mean ± S.E., $n = 3$. #, $p < 0.05$ and §, $p < 0.005$ when compared with LXA4; *, $p < .025$ when compared with RvD1.

DISCUSSION

D series resolvins and their aspirin-triggered epimers are potent DHA-derived local mediators that are generated during the resolution phase of inflammation and exhibit potent anti-inflammatory actions *in vivo* (5, 15, 31). Because several D series resolvins are generated *in vivo*, the identity and stereochemical configuration of the biologically active RvD1 remained to be established. Given the emerging importance of inflammatory resolution as a homeostatic mechanism as well as terrain for new therapeutic targets (5, 34), we determined the complete stereochemical assignments of bioactive RvD1 and AT-RvD1 and directly compared their bioactivities as well as identified further metabolic products of inactivation.

RvD1 and AT-RvD1 prepared via total organic synthesis in stereochemically pure form displayed similar NMR spectra (Fig. 2). However, because these molecules differ only in the stereochemistry of the 17-hydroxyl group, they are diastereomers, and as such should exhibit some differences in physical properties. Indeed, RP-HPLC and LC-MS/MS-based analyses of enantiomerically pure synthetic RvD1 and AT-RvD1 (Fig. 3*A*) showed that the two compounds are distinguishable by retention time, with AT-RvD1 eluting ~1.2 min earlier. Along these lines, MS/MS analysis of both compounds yielded essentially identical fragmentation patterns (Fig. 3, *B–D*).

RvD1 and AT-RvD1 are derived from DHA, and their proposed biosynthetic pathways are shown in Fig. 1 to involve sequential oxygenations initiated by 15-LOX or aspirin acetylated cyclooxygenase-2 followed by 5-LOX. 5-LOX is known to generate 5*S*-hydroperoxyeicosatetraenoic acid predominantly in the *S* configuration, followed by *trans* epoxidation to produce leukotriene A_4 from arachidonic acid (35). Because this pathway appeared to be shared in RvD1 biosynthesis (5), the stereochemistry of RvD1 and role of epoxide intermediate were proposed (Fig. 1). The results

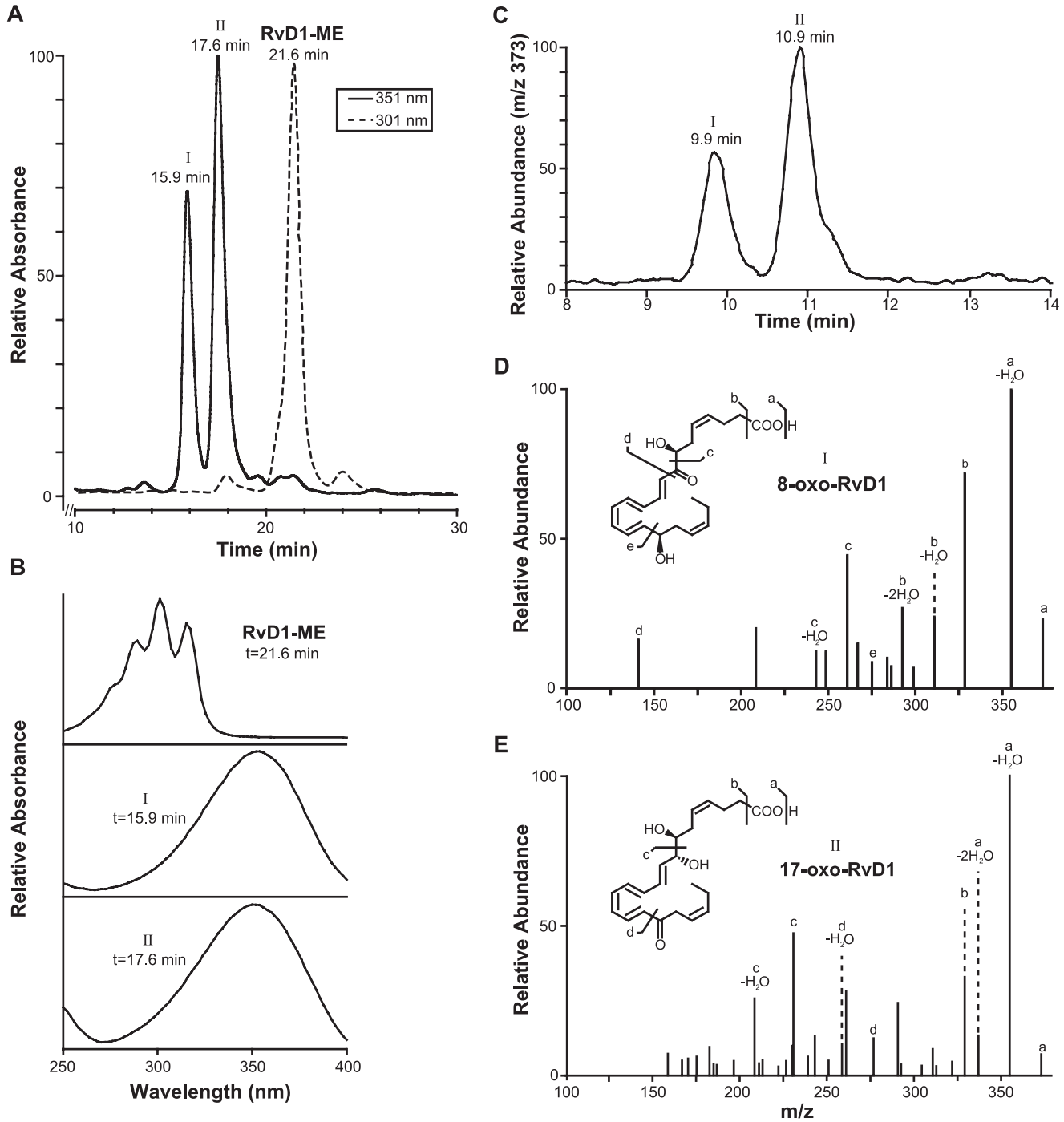

FIGURE 8. **RvD1 further metabolites.** RvD1-ME (5 μg) was incubated with EOR (5 μg) at 37 °C (0.1 M Tris-HCl, pH 7.4, 10 mM NAD^+, 100 μl of total volume) for 2 h. The incubation was then extracted and analyzed by RP-HPLC. *A*, RP-HPLC chromatogram of oxo-RvD1-ME metabolites monitored at $\lambda_{max} = 351$ (*solid line*) and RvD1-ME monitored at $\lambda_{max} = 301$ (*dotted line*). *B*, UV absorbance spectra of major peaks at 21.6, 15.9, and 17.6 min. *C*, selected ion chromatogram (*m/z* 373) for mono oxo-containing products of RvD1. *D*, MS/MS analysis of compound I at *m/z* 373. *E*, MS/MS analysis of compound II at *m/z* 373.

presented here show that the major isomer of biogenic RvD1 matches the physical characteristics of the RvD1 prepared in isomerically pure form by total organic synthesis thereby defining the stereochemistry of RvD1 as 7*S*,8*R*,17*S*-trihydroxy-4*Z*,9*E*,11*E*,13*Z*,15*E*,19*Z*-docosahexaenoic acid. Although RvD1 can be a product of transcellular biosynthesis *in vivo*, requiring at least two distinct enzymes (5, 15), our results demonstrate that RvD1 can also be generated *in vitro* in a one-pot single enzyme incubation (17). The ability of LOX to oxygenate DHA at both the 17 and 7 positions illustrates the positional flexibility of this enzyme, a finding that is in corroboration with earlier studies showing that 15-LOX can accept substrates with standard (methyl terminus entry) orientation as well as the inverse orientation (carboxyl terminus entry) (36).

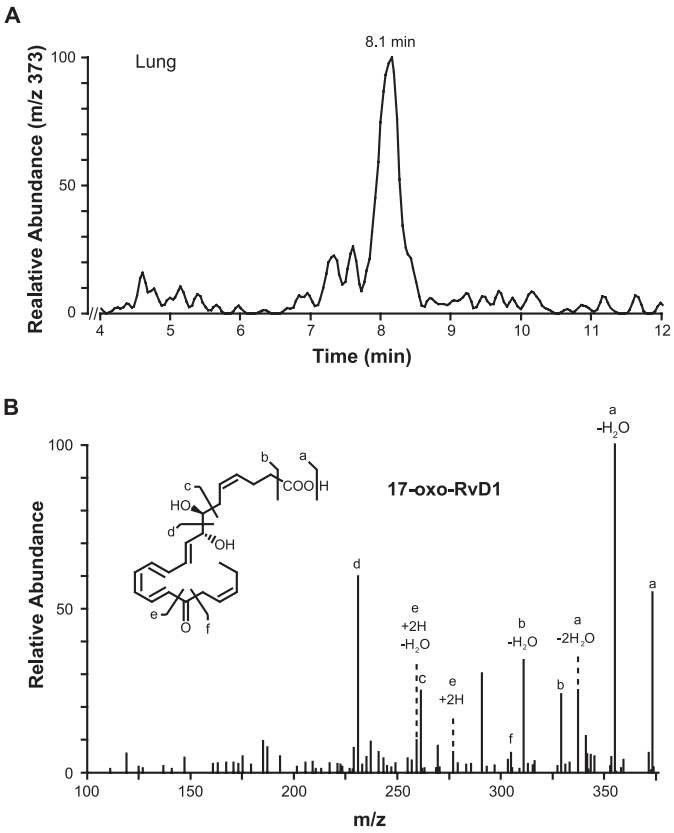

FIGURE 9. **Lung generation of 17-oxo-RvD1.** Zymosan A (1 mg/ml) was injected intraperitoneally into 6- to 8-week-old male FVB mice. After 4 h, the lungs were harvested and homogenized. The homogenized tissue was then incubated with RvD1 (100 ng) and NAD^+ (1.0 mM) for 20 min at 37 °C. The incubation was then extracted and analyzed via LC-MS/MS. *A*, selected ion chromatogram (*m/z* 373) for mono oxo-RvD1 products. *B*, MS/MS analysis of the major peak at 8.1 min at *m/z* 373.

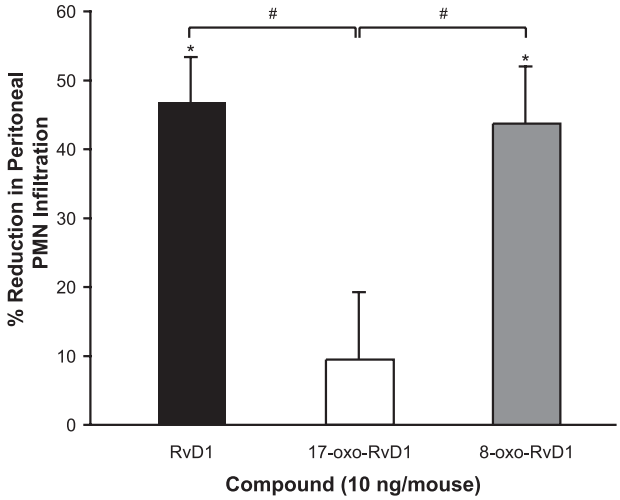

FIGURE 10. **RvD1 inactivation metabolites in acute inflammation.** Each compound (RvD1-ME, 8-oxo-RvD1-ME, and 17-oxo-RvD1-ME) was injected by intravenous bolus injection (10 ng/100 μl of sterile saline) via the tail vein of 6- to 8-week-old male FVB mice followed by peritoneal injection of zymosan A (1 mg/ml). Peritoneal lavages were collected (4 h) and were enumerated. Reduction of PMN infiltration was determined by direct comparison with zymosan plus vehicle control (100 μl of sterile saline). Values represent mean ± S.E., $n = 5–6$; *, $p < 0.05$ as compared with vehicle control; #, $p < 0.05$ as compared with 17-oxo-RvD1-ME.

Based on the stereochemical assignment of RvD1 and results of biosynthesis, RvD1 formation was proposed to be via enzymatic hydrolysis of a *trans*-7,8-epoxide-containing intermediate (5, 15). Because it is theoretically possible that RvD1 biosynthesis could also proceed via a 16,17-epoxide intermediate followed by a subsequent 1,10 addition (see "*Additional Pathway*" in Fig. 1), we determined whether an epoxide intermediate was involved in RvD1. Identification of methoxy-RvD1-trapping products in both human leukocyte suspensions and isolated DHA and LOX incubations demonstrated that the major pathway involved in this step of the biosynthesis involves an epoxide intermediate. Acidic methanol trapping of the single enzyme (LOX) incubations used to generate RvD1 in Fig. 4 also yielded epoxide-derived trapping products likely generated via a carbonium cation intermediate (37, 38) as the major products (Fig. 5).

Earlier reports demonstrated that the D series resolvins as well as their aspirin-triggered counterparts reduce PMN infiltration by ~40% at a 100-ng dose *in vivo*, a decrease that was comparable to that obtained with indomethacin, a traditional and widely used non-steroidal anti-inflammatory drug (5, 15). Both RvD1 and AT-RvD1 demonstrated a dose-dependent decrease in PMN infiltration with a maximal inhibition of ~35% occurring at the 10- to 100-ng dose (Fig. 6*B*). Significant differences in potency between these two epimers were not observed suggesting that the two share a common site of action on PMNs. In contrast, although RvD1 and AT-RvD1 were equally efficacious in decreasing total leukocytic infiltration, AT-RvD1 proved to be statistically more potent at the 10-ng dose level than RvD1 (Fig. 6*B*). The leukocytic infiltration after 4 h *in vivo* was composed of PMNs (~70%) and monocytes (~30%). Because AT-RvD1 and RvD1 demonstrated equal actions on PMNs, the results shown in Fig. 6 suggest that the two may have different actions on monocytes, a finding that might be relevant given the prominent role of the monocyte/macrophage lineage in inflammation and its resolution (reviewed in Ref. 7) or may reflect the different local levels of these two epimers.

RvD1 and AT-RvD1 are generated locally in response to inflammatory stimuli (5, 15), where they possess potent anti-inflammatory action. This inflammatory milieu is dynamic, and the presence of several cell types, including activated PMNs and monocytes, suggests that both RvD1 and AT-RvD1 may be subject to further metabolism. The arachidonic acid cousin of RvD1, LXA_4, is inactivated by an EOR via oxidation to 15-oxo-LXA_4 (39). Interestingly, aspirin-triggered LXA_4, differing from LXA_4 only in the stereochemical configuration at carbon 15 (*S versus R*, respectively), resists inactivation by this EOR (40). Our results in Fig. 6 show that AT-RvD1 is more resistant to catalysis by the EOR than RvD1. This finding follows the trend found earlier with LXA_4 and aspirin-triggered LXA_4 suggesting that this EOR may preferentially act on *S*-configured ω-proximal hydroxyl groups rather than their *R*-configured counterparts. Chromatographic analysis in Fig. 8 showed that both 8-oxo-RvD1 and 17-oxo-RvD1 were generated, a finding not observed with LXA_4. The EOR utilized here has been demonstrated to act preferentially at hydroxyl groups at the ω-6 position and not at α-proximal hydroxyls such as 5-hydroxyeicosatetraenoic acid, thereby implicating the ω terminus as a recognition

domain for the enzyme (41). Because RvD1 possesses an elongated carbon chain with an additional olefinic moiety at the α terminus, its conversion to 8-oxo-RvD1 suggests that these structural features may also serve as a recognition domain for the enzyme.

The finding that 17-oxo-RvD1 is biologically inactive (Fig. 10) is consistent with the role of these EORs as inactivating enzymes (29, 33). Because most lipid mediators are autocoids that are generated, act locally, and are inactivated quickly, these findings identify this conversion from RvD1 to 17-oxo-RvD1 as a structure-activity relationship for potential inactivation *in vivo* as observed here with lung that may regulate the temporal and local actions of RvD1.

The importance of dietary DHA in human health and disease has been appreciated for over 30 years (8). The molecular basis of its actions has begun to be elucidated with the identification of protectin D1, a dihydroxy enzymatic product with anti-inflammatory and neuroprotective actions (31). In addition to the anti-inflammatory properties demonstrated here, RvD1 is generated in response to brain ischemia-reperfusion and 15-LOX pathways are important in epithelial wound healing (42), suggesting that the D series resolvins are also likely to contribute to the well appreciated protective actions of DHA. The total organic synthesis of one of these, resolvin D2 (RvD2), was reported (43) and is a key step in further characterization of the biological roles of the D series resolvins. Our results presented here establish the complete stereochemistry of RvD1 and its aspirin-triggered epimer AT-RvD1, document their potent anti-inflammatory actions and identify key features of their structure-activity relationships and biological inactivation *in vivo*.

Acknowledgment—We thank Mary Halm Small for assistance with manuscript preparation.

REFERENCES

1. Burr, G. O., and Burr, M. M. (1929) *J. Biol. Chem.* **82,** 345–367
2. Gallin, J. I., Snyderman, R., Fearon, D. T., Haynes, B. F., and Nathan, C. (eds) (1999) *Inflammation: Basic Principles and Clinical Correlates*, 3rd Ed., Lippincott Williams & Wilkins, Philadelphia
3. Majno, G., and Joris, I. (2004) *Cells, Tissues, and Disease: Principles of General Pathology*, 2nd Ed., Oxford University Press, New York
4. Serhan, C. N., Clish, C. B., Brannon, J., Colgan, S. P., Chiang, N., and Gronert, K. (2000) *J. Exp. Med.* **192,** 1197–1204
5. Serhan, C. N., Hong, S., Gronert, K., Colgan, S. P., Devchand, P. R., Mirick, G., and Moussignac, R.-L. (2002) *J. Exp. Med.* **196,** 1025–1037
6. Bannenberg, G. L., Chiang, N., Ariel, A., Arita, M., Tjonahen, E., Gotlinger, K. H., Hong, S., and Serhan, C. N. (2005) *J. Immunol.* **174,** 4345–4355
7. Serhan, C. N., and Savill, J. (2005) *Nat. Immunol.* **6,** 1191–1197
8. Bang, H. O., Dyerberg, J., and Hjørne, N. (1976) *Acta Med. Scand.* **200,** 69–73
9. Simopoulos, A. P. (1999) *Am. J. Clin. Nutr.* **70,** (suppl.) 560S–569S
10. Belluzzi, A., Brignola, C., Campieri, M., Pera, A., Boschi, S., and Miglioli, M. (1996) *N. Engl. J. Med.* **334,** 1557–1560
11. GISSI-Prevenzione Investigators (1999) *Lancet* **354,** 447–455
12. Albert, C. M., Campos, H., Stampfer, M. J., Ridker, P. M., Manson, J. E., Willett, W. C., and Ma, J. (2002) *N. Engl. J. Med.* **346,** 1113–1118
13. Bazan, N. G. (1990) in *Nutrition and the Brain* (Wurtman, R. J., and Wurtman, J. J., eds) pp. 1–22, Raven Press, New York
14. Salem, N., Jr., Litman, B., Kim, H.-Y., and Gawrisch, K. (2001) *Lipids* **36,** 945–959
15. Hong, S., Gronert, K., Devchand, P., Moussignac, R.-L., and Serhan, C. N. (2003) *J. Biol. Chem.* **278,** 14677–14687
16. Hong, S., Tjonahen, E., Morgan, E. L., Yu, L., Serhan, C. N., and Rowley, A. F. (2005) *Prostaglandins Other Lipid Mediat.* **78,** 107–116
17. Serhan, C. N. (2004) U. S. Patent Application Publication No. 2004/0116408 A1, published June 17, 2004
18. Serhan, C. N., and Clish, C. B. (2003) U.S. Patent No. 6,670,396 B2, December 30, 2003
19. Calder, P. C. (2001) *Lipids* **36,** 1007–1024
20. Lu, Y., Hong, S., Gotlinger, K., and Serhan, C. N. (2006) *ScientificWorldJournal* **6,** 589–614
21. Lu, Y., Hong, S., Tjonahen, E., and Serhan, C. N. (2005) *J. Lipid Res.* **46,** 790–802
22. Serhan, C. N. (1990) *Methods Enzymol.* **187,** 167–175
23. Robinson, K. A., Candal, F. J., Scott, N. A., and Ades, E. W. (1995) *Angiology* **46,** 107–113
24. Collard, C. D., Park, K. A., Montalto, M. C., Alapati, S., Buras, J. A., Stahl, G. L., and Colgan, S. P. (2002) *J. Biol. Chem.* **277,** 14801–14811
25. Lennon, P. F., Taylor, C. T., Stahl, G. L., and Colgan, S. P. (1998) *J. Exp. Med.* **188,** 1433–1443
26. Parkos, C. A., Delp, C., Arnaout, M. A., and Madara, J. L. (1991) *J. Clin. Invest.* **88,** 1605–1612
27. Lawrence, D. W., Bruyninckx, W. J., Louis, N. A., Lublin, D. M., Stahl, G. L., Parkos, C. A., and Colgan, S. P. (2003) *J. Exp. Med.* **198,** 999–1010
28. Perretti, M., and Getting, S. J. (2003) in *Inflammation Protocols* (Winyard, P. G., and Willoughby, D. A., eds) pp. 139–146, Humana, Totowa, NJ
29. Clish, C. B., Levy, B. D., Chiang, N., Tai, H.-H., and Serhan, C. N. (2000) *J. Biol. Chem.* **275,** 25372–25380
30. Chiang, N., Takano, T., Clish, C. B., Petasis, N. A., Tai, H.-H., and Serhan, C. N. (1998) *J. Pharmacol. Exp. Ther.* **287,** 779–790
31. Marcheselli, V. L., Hong, S., Lukiw, W. J., Hua Tian, X., Gronert, K., Musto, A., Hardy, M., Gimenez, J. M., Chiang, N., Serhan, C. N., and Bazan, N. G. (2003) *J. Biol. Chem.* **278,** 43807–43817
32. Serhan, C. N., Fiore, S., Brezinski, D. A., and Lynch, S. (1993) *Biochemistry* **32,** 6313–6319
33. Tai, H. H., Ensor, C. M., Tong, M., Zhou, H., and Yan, F. (2002) *Prostaglandins Other Lipid Mediat.* **68–69,** 483–493
34. Gilroy, D. W., Lawrence, T., Perretti, M., and Rossi, A. G. (2004) *Nat. Rev. Drug Discov.* **3,** 401–416
35. Borgeat, P., and Samuelsson, B. (1979) *Proc. Natl. Acad. Sci. U. S. A.* **76,** 2148–2152
36. Schwarz, K., Borngräber, S., Anton, M., and Kuhn, H. (1998) *Biochemistry* **37,** 15327–15335
37. Serhan, C. N. (1994) *Biochim. Biophys. Acta* **1212,** 1–25
38. Corey, E. J., and Mehrotra, M. M. (1986) *Tetrahedron Lett.* **27,** 5173–5176
39. Maddox, J. F., and Serhan, C. N. (1996) *J. Exp. Med.* **183,** 137–146
40. Serhan, C. N., Maddox, J. F., Petasis, N. A., Akritopoulou-Zanze, I., Papayianni, A., Brady, H. R., Colgan, S. P., and Madara, J. L. (1995) *Biochemistry* **34,** 14609–14615
41. Bergholte, J. M., Soberman, R. J., Hayes, R., Murphy, R. C., and Okita, R. T. (1987) *Arch. Biochem. Biophys.* **257,** 444–450
42. Gronert, K., Maheshwari, N., Khan, N., Hassan, I. R., Dunn, M., and Schwartzman, M. L. (2005) *J. Biol. Chem.* **280,** 15267–15278
43. Rodriguez, A. R., and Spur, B. W. (2004) *Tetrahedron Lett.* **45,** 8717–8720

Resolvin D1 and Its Aspirin-triggered 17*R* Epimer: STEREOCHEMICAL ASSIGNMENTS, ANTI-INFLAMMATORY PROPERTIES, AND ENZYMATIC INACTIVATION

Yee-Ping Sun, Sungwhan F. Oh, Jasim Uddin, Rong Yang, Katherine Gotlinger, Eric Campbell, Sean P. Colgan, Nicos A. Petasis and Charles N. Serhan

J. Biol. Chem. 2007, 282:9323-9334.
doi: 10.1074/jbc.M609212200 originally published online January 23, 2007
